



Deeply Virtual Compton Scattering off proton and neutron from deuterium with CLAS12 at Jefferson Laboratory

Adam HOBART on behalf of CLAS Collaboration

EINN 2023, Paphos, Cyprus





GPDs

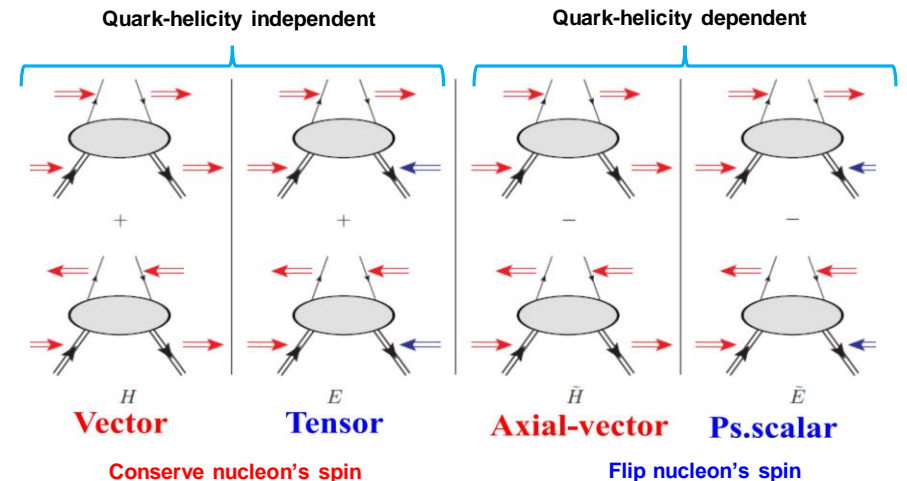
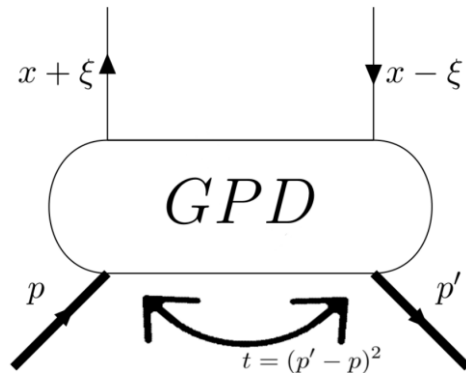
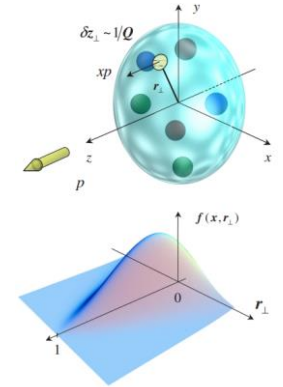
Belitsky, Radyushkin, Physics Reports, 2005

- QCD at low energies: non perturbative regime
 - Need **structure functions** to describe nucleon structure

GPDs

Correlation of transverse position and longitudinal momentum of partons in the nucleon & the spin structure - through Ji's sum rule X. Ji, Phy.Rev.Lett.78,610(1997)

- GPDs can be accessed through **exclusive leptonproduction reactions**
- At leading order QCD, chiral-even (quark helicity is conserved), quark sector: 4 **GPDs** for each quark flavor H, \tilde{H}, E and \tilde{E}
- GPDs depend on x, ξ and $t = (p' - p)^2$





Why are GPDs important?

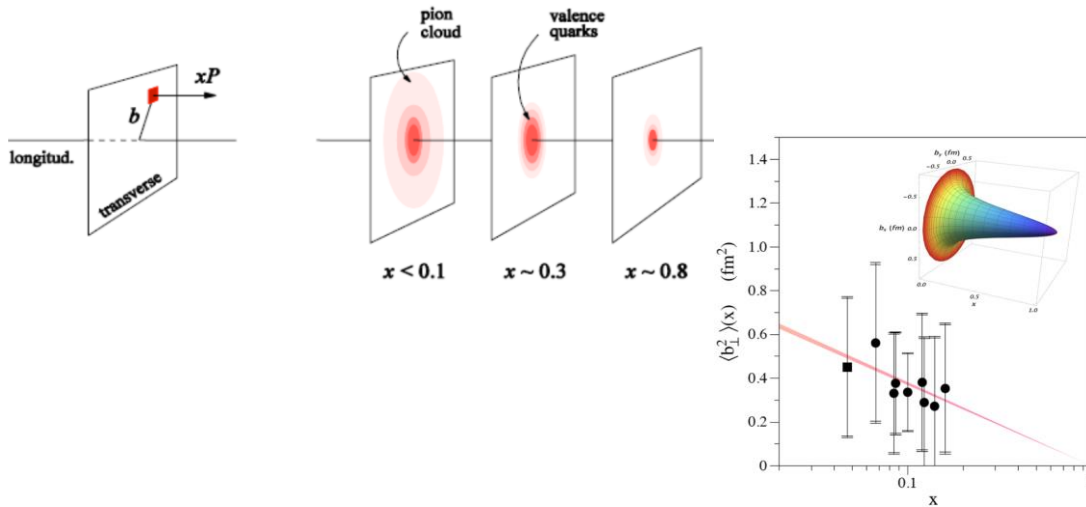
- GPDs: Fourier transforms of non-local, non-diagonal QCD operators

Nucleon tomography

M. Burkardt, PRD 62, 71503 (2000)

$$q(x, b_{\perp}) = \int_0^{\infty} \frac{d^2 \Delta_{\perp}}{(2\pi)^2} e^{i\Delta_{\perp} b_{\perp}} H(x, 0, -\Delta_{\perp}^2)$$

$$\Delta q(x, b_{\perp}) = \int_0^{\infty} \frac{d^2 \Delta_{\perp}}{(2\pi)^2} e^{i\Delta_{\perp} b_{\perp}} \tilde{H}(x, 0, -\Delta_{\perp}^2)$$



R. Dupré, M. Guidal, M.Vanderhaeghen, PRD95, 011501 (2017)

Quark angular momentum

X. Ji, Phy.Rev.Lett.78,610(1997)

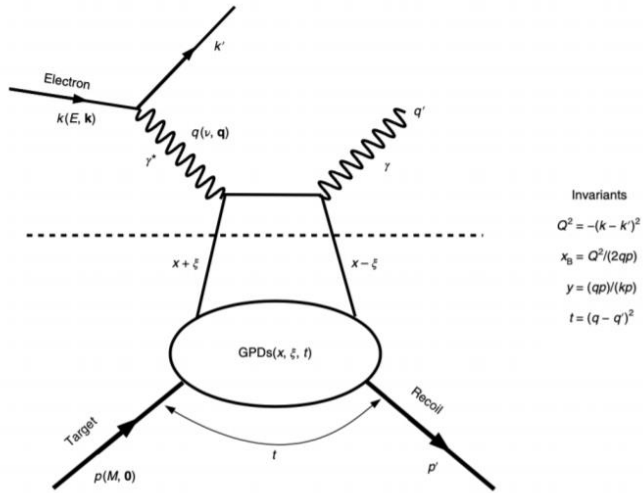
$$\frac{1}{2} \int_{-1}^1 x dx (H(x, \xi, t=0) + E(x, \xi, t=0)) = J = \frac{1}{2} \Delta\Sigma + \Delta L$$

$$\text{Nucleon spin: } \frac{1}{2} = \frac{1}{2} \Delta\Sigma + \Delta L + \Delta G$$

- The intrinsic spin of the quarks can not explain the origin of the spin of the nucleon (**nucleon Spin Crisis**)
- Intrinsic spin of the gluons
- GPDs: quantify the contribution of orbital angular momentum of quarks to the nucleon spin



Deeply Virtual Compton Scattering of leptons off nucleons



- DVCS allows access to 4 complex GPDs-related quantities:
 - Compton Form Factors (x, ξ, t) (CFFs)

$$\mathcal{H} = \sum_q e_q^2 \left\{ i \pi [H^q(\xi, \xi, t) - H^q(-\xi, \xi, t)] + \mathcal{P} \int_{-1}^1 dx H^q(x, \xi, t) \left[\frac{1}{\xi - x} - \frac{1}{\xi + x} \right] \right\}$$

- x can not be accessed experimentally by DVCS: Models needed to map the x dependence

$$\sigma(eN \rightarrow eN\gamma) = \left[\text{DVCS} + \text{Bethe-Heitler (BH)} \right]^2$$

BH is purely electromagnetic and parametrised by FFs

- Experimentally measured observables:
 - Sensitive to the DVCS-BH interference part (linear in CFFs)
 - Should have: Beam polarized and/or target polarized
 - Access to a combinations of CFFs
 - The separation of CFFs requires the measurement of several observables
 - Depending on the target (proton or neutron): different sensitivity to the CFFs (GPDs)
 - The flavor separation of GPDs requires measurements on both nucleons

$$(H, E)_u(\xi, \xi, t) = \frac{9}{15} [4(H, E)_p(\xi, \xi, t) - (H, E)_n(\xi, \xi, t)]$$

$$(H, E)_d(\xi, \xi, t) = \frac{9}{15} [4(H, E)_n(\xi, \xi, t) - (H, E)_p(\xi, \xi, t)]$$



Different contributions from F_1 and F_2 for the different nucleons

Polarized beam, unpolarized target

$$\Delta\sigma_{LU} \sim \sin(\phi) \Im\{F_1 \mathbf{H} + \xi(F_1 + F_2) \tilde{\mathbf{H}} - k F_2 \mathbf{E} + \dots\}$$

Unpolarized beam, polarized target

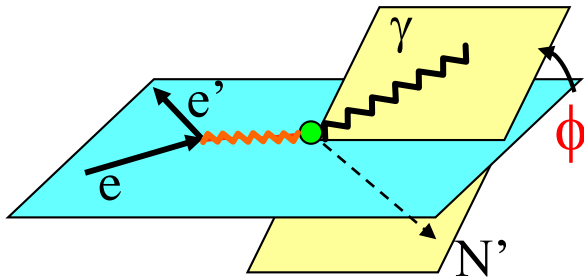
$$\Delta\sigma_{UL} \sim \sin(\phi) \Im\left\{F_1 \tilde{\mathbf{H}} + \xi(F_1 + F_2) \left(\mathbf{H} + \frac{x_b}{2} \mathbf{E}\right) - \xi k F_2 \tilde{\mathbf{E}}\right\}$$

polarized beam, longitudinal polarized target

$$\Delta\sigma_{LL} \sim (A + B \cos(\phi)) \Re\{F_1 \tilde{\mathbf{H}} + \xi(F_1 + F_2) \left(\mathbf{H} + \frac{x_b}{2} \mathbf{E}\right) + \dots\}$$

unpolarized beam, transverse polarized target

$$\Delta\sigma_{UT} \sim \cos(\phi) \sin(\phi_s - \phi) \Im\{k(F_2 \mathbf{H} - F_1 \mathbf{E}) + \dots\}$$



Observable	Proton	Neutron
$\Delta\sigma_{LU}$	$\Im\{\mathbf{H}_p, \tilde{\mathbf{H}}_p, E_p\}$	$\Im\{H_n, \tilde{H}_n, E_n\}$
$\Delta\sigma_{UL}$	$\Im\{\mathbf{H}_p, \tilde{\mathbf{H}}_p\}$	$\Im\{\mathbf{H}_n, E_n\}$
$\Delta\sigma_{LL}$	$\Re\{\mathbf{H}_p, \tilde{\mathbf{H}}_p\}$	$\Re\{\mathbf{H}_n, E_n\}$
$\Delta\sigma_{UT}$	$\Im\{\mathbf{H}_p, E_p\}$	$\Im\{\mathbf{H}_n\}$

e.g. (in experiment)
$$\Delta\sigma_{LU} = \frac{1}{Pol.} \times \frac{N^+ - N^-}{N^+ + N^-}$$



Different contributions from F_1 and F_2 for the different nucleons

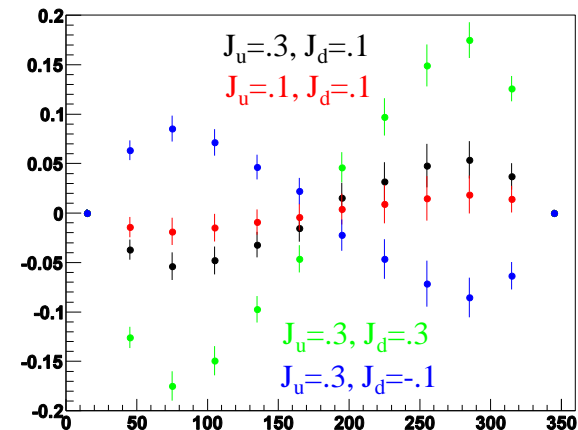
- **DVCS with an unpolarized deuterium target :**
- Scattering off neutron (nDVCS): GPD **E**
 - Determination of Ji sum rule
 - Contribution of orbital angular momentum of quarks to the nucleon spin

$$\frac{1}{2} \int_{-1}^1 x dx (H(x, \xi, t=0) + E(x, \xi, t=0)) = J = \frac{1}{2} \Delta \Sigma + \Delta L$$

- Scattering off proton (pDVCS): GPD **H**
 - Quantify medium effects
 - Essential for the extraction of BSA of a “free” neutron (deconvoluting medium effect via comparison with DVCS on hydrogen target)
- The BSA for nDVCS:
 - is complementary to the TSA for pDVCS on transverse target, aiming at E
 - depends strongly on the kinematics \rightarrow wide coverage needed
 - is smaller than for pDVCS \rightarrow more beam time needed to achieve reasonable statistics

Observable	Proton	Neutron
$\Delta\sigma_{LU}$	$\Im\{\mathbf{H}_p, \tilde{\mathbf{H}}_p, E_p\}$	$\Im\{H_n, \tilde{H}_n, E_n\}$
$\Delta\sigma_{UL}$	$\Im\{\mathbf{H}_p, \tilde{\mathbf{H}}_p\}$	$\Im\{\mathbf{H}_n, E_n\}$
$\Delta\sigma_{LL}$	$\Re\{\mathbf{H}_p, \tilde{\mathbf{H}}_p\}$	$\Re\{\mathbf{H}_n, E_n\}$
$\Delta\sigma_{UT}$	$\Im\{\mathbf{H}_p, E_p\}$	$\Im\{\mathbf{H}_n\}$

Model predictions (VGG) for different values of quarks' angular momentum



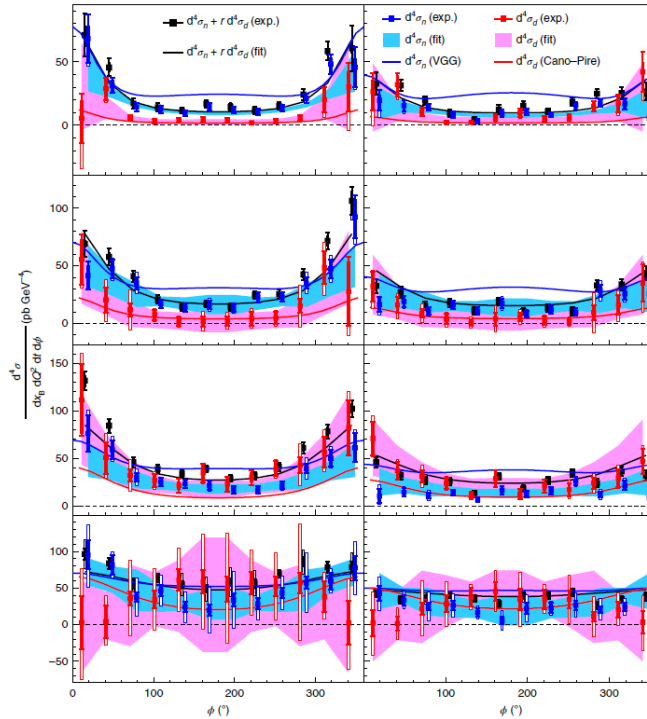


Deeply Virtual Compton Scattering with an unpolarized deuterium target

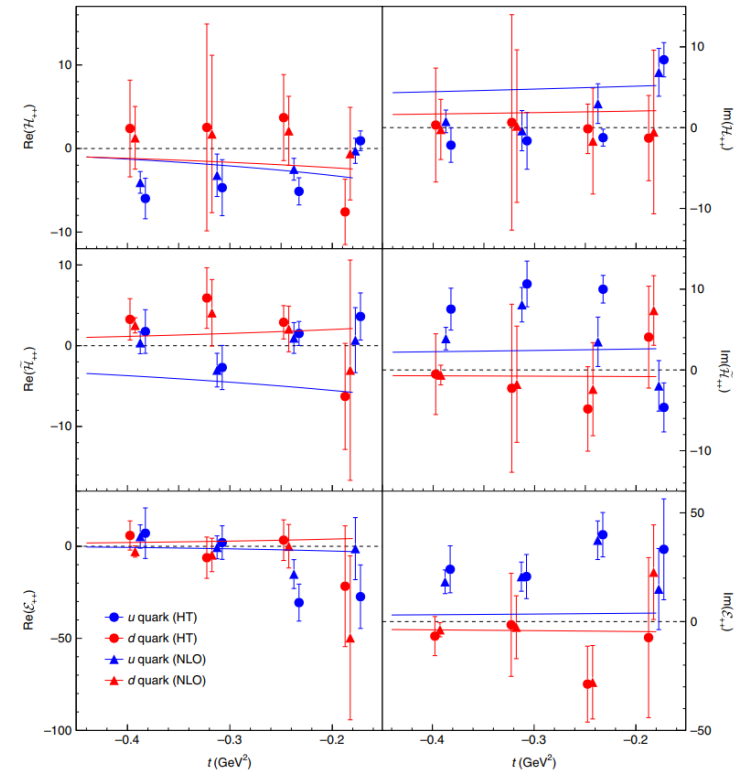
- Previous pioneering measurement of nDVCS (Jlab Hall A @ 6 GeV)
 - Beam-energy « Rosenbluth » separation of nDVCS CS using an LD2 target and two different beam energies
 - First observation of non-zero nDVCS CS

- No neutron detection $D(e, e'\gamma)X - H(e, e'\gamma)X = n(e, e'\gamma)n + d(e, e'\gamma)d + \dots$

One measured kinematical point:
 $Q^2=1.9 \text{ GeV}^2$ and $x_B=0.36$



+data from: Mazouz, M. et al. Phys. Rev. Lett. 99, 242501 (2007).



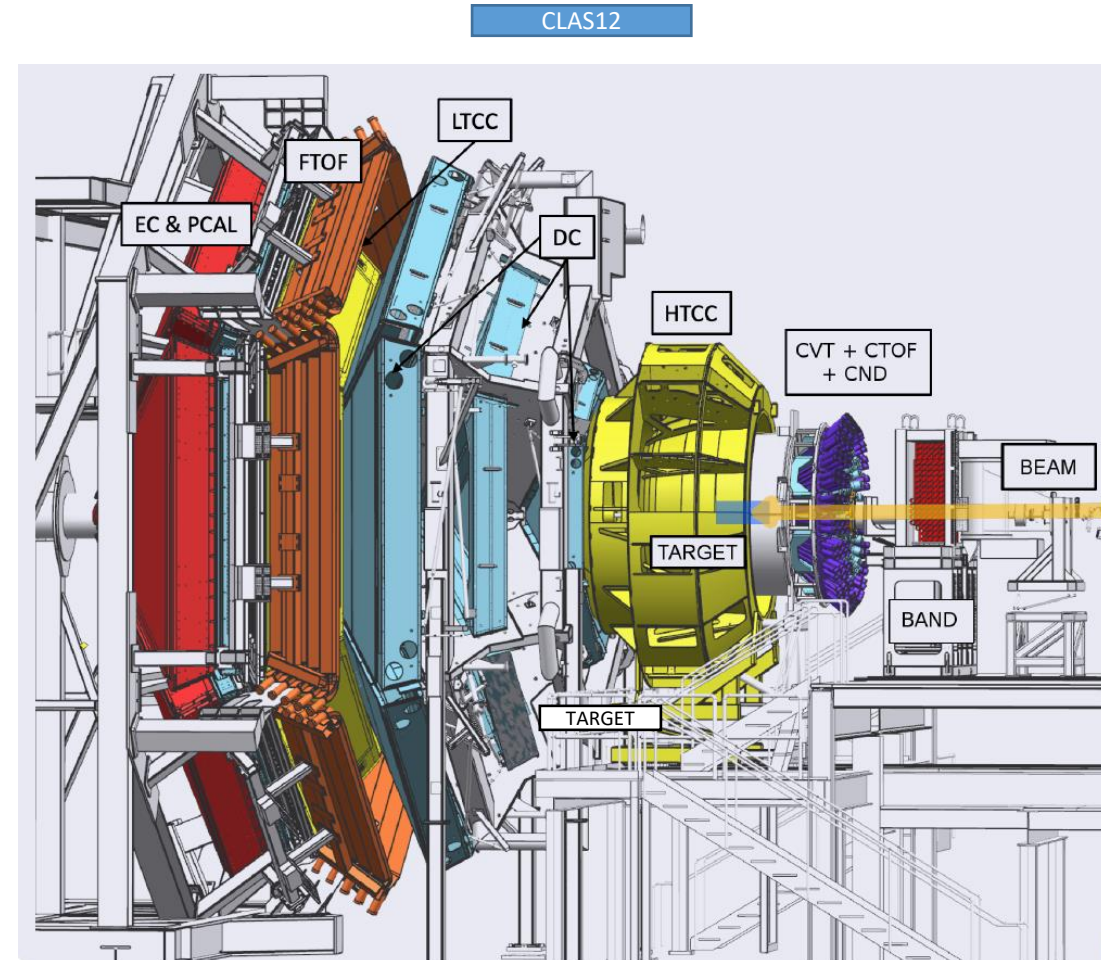
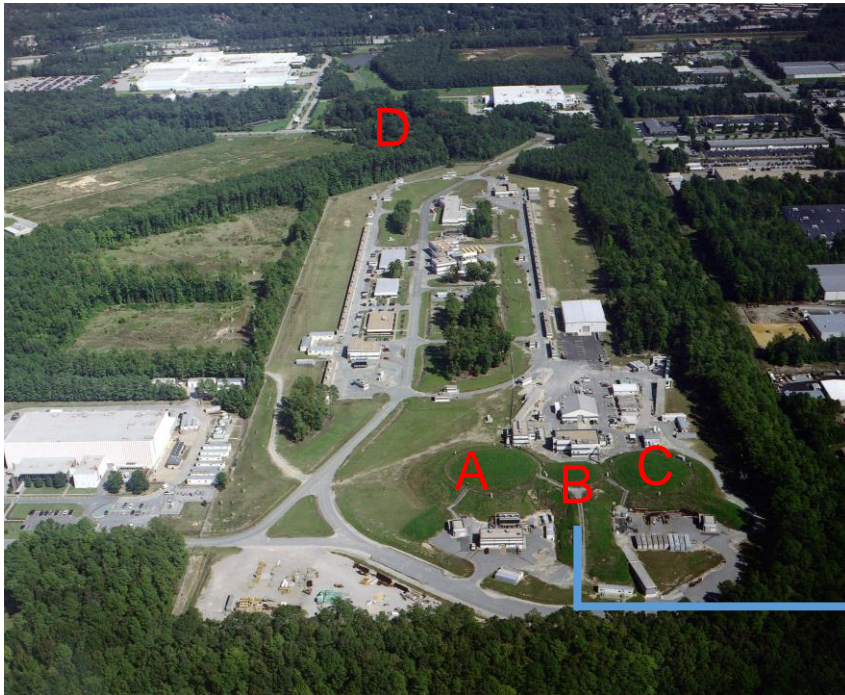
Benali, M., Desnault, C., Mazouz, M. et al. Nat. Phys. 16, 191–198 (2020)



The CEBAF and CLAS at Jefferson Laboratory

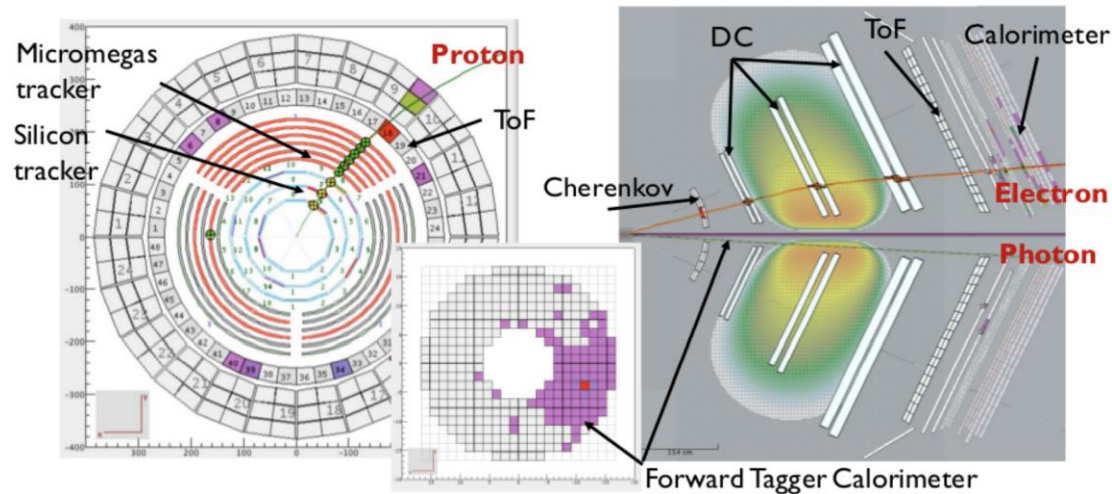
Continuos Electron Beam Accelerator Facility

- Up to 12 GeV electrons
- Two anti-parallel linacs, with recirculating arcs on both ends
- 4 experimental halls



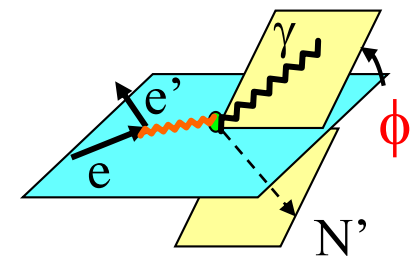
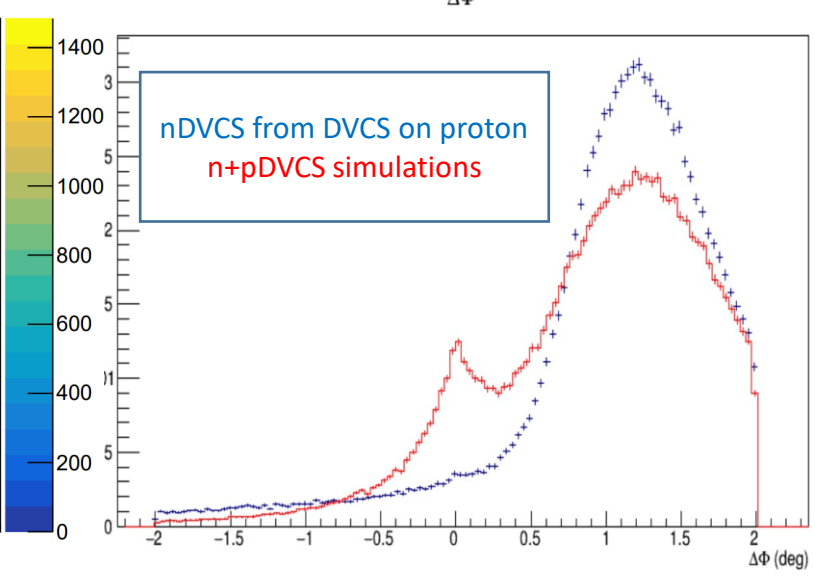
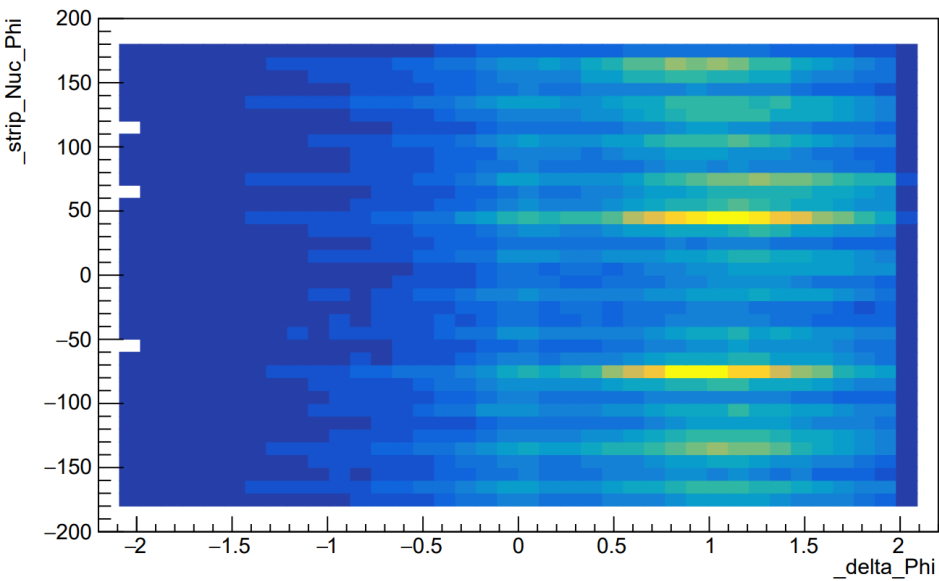


- A 10.6/10.4/10.2 GeV electron beam
 - With an average polarization of 86%
 - Scattering off an unpolarized Liquid Deuterium target of 5 cm length
- The exclusivity of the event is insured by:
 - **Electron detection**: Cerenkov detector, drift chambers and electromagnetic calorimeter
 - **Photon detection**: sampling calorimeter or a small PbWO₄-calorimeter close to the beamline
 - **Proton detection**: Silicon and Micromegas detector OR **Neutron detection**: Central Neutron Detector
- For Neutron Detection:
 - Machine Learning techniques are applied to improve the Identification and reduce charged particle contamination





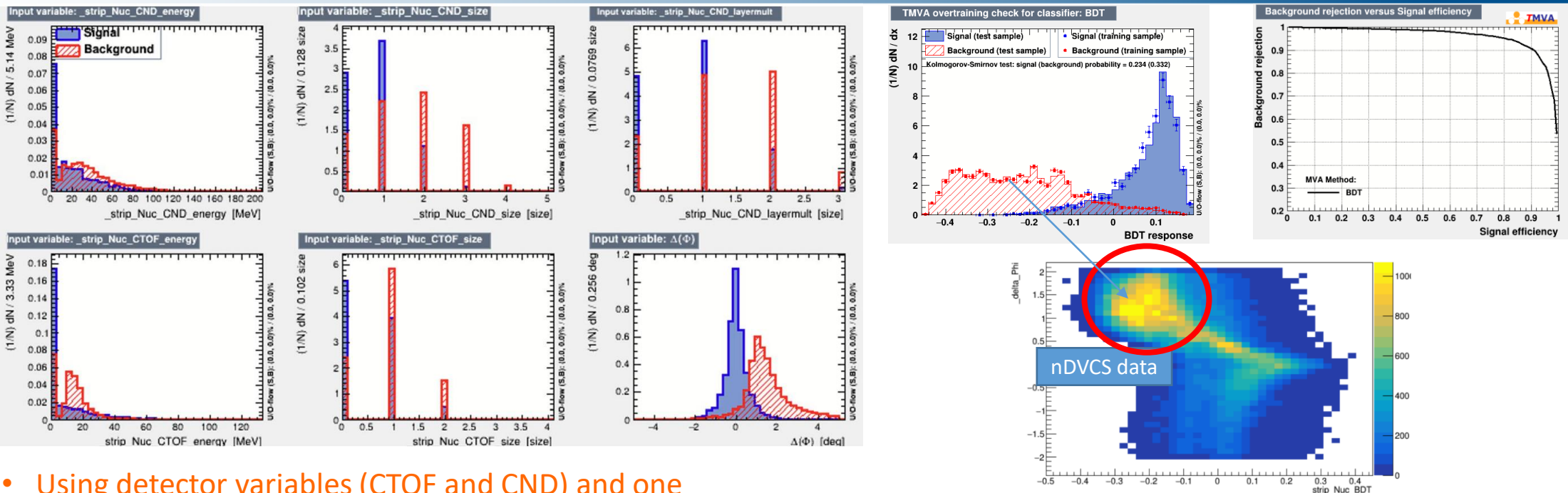
- The tracking of the CVT is neither 100% efficient nor uniform
- In the dead regions of the CVT **protons** have no associated track and thus can be **misidentified as neutrons**
- Protons roughly account for more than **>40% contamination in the “nDVCS”** signal sample Current approach, based on Machine Learning & Multi-Variate Algorithms:
 - We reconstruct nDVCS from DVCS experiment on proton requiring neutron PID : **selected neutron are misidentified protons**
 - We use this sample to determine the characteristics of fake neutrons in low- and high-level reconstructed variables
 - Based on those characteristics we subtract the fake neutrons contamination from nDVCS
 - As a « signal » sample in the training of the ML we use $ep \rightarrow en\pi^+$ events from DVCS experiment on proton



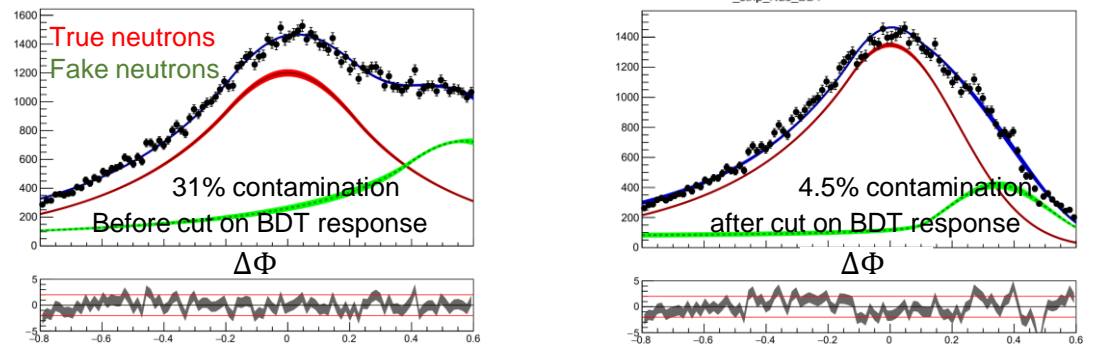


Improving the neutron selection with ML techniques

Under internal review

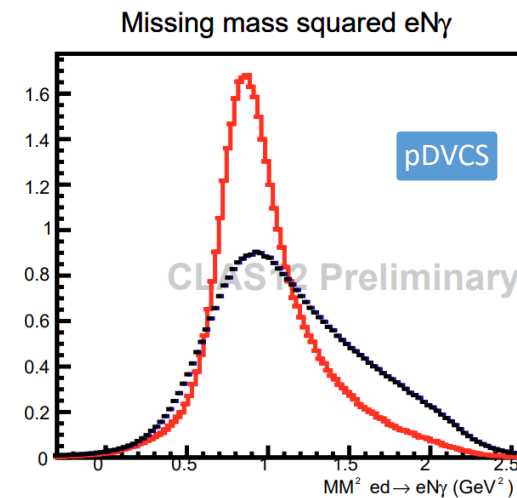
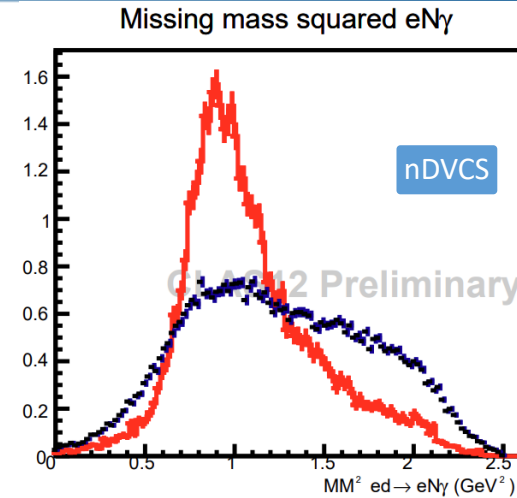


- Using detector variables (CTOF and CND) and one exclusivity variable ($\Delta\Phi$)
- Directly trained on data
- Better optimization of signal to background ratio than straight cuts
- Few percent irreducible contamination corrected for in the final BSA





- The nDVCS (pDVCS) final state is selected with the following exclusivity criteria: (N:nucleon)
 - Missing mass
 - $e d \rightarrow e N \gamma X$
 - $e N \rightarrow e N \gamma X$
 - $e N \rightarrow e N X$
 - Missing momentum
 - $e d \rightarrow e N \gamma X$
 - $\Delta\Phi, \Delta t, \theta(\gamma, X)$
 - Difference between two ways of calculating Φ and t
 - Cone angle between measured and reconstructed photon
- Exclusivity selection is optimized with a 4-D χ^2 -like distribution including $\Delta\Phi, \Delta t, \theta(\gamma, X)$ and missing mass $e N \rightarrow e N X$



- Simulation (Red circle)
- Data with π^0 contamination (Black circle)

π^0 background contamination is estimated using simulations



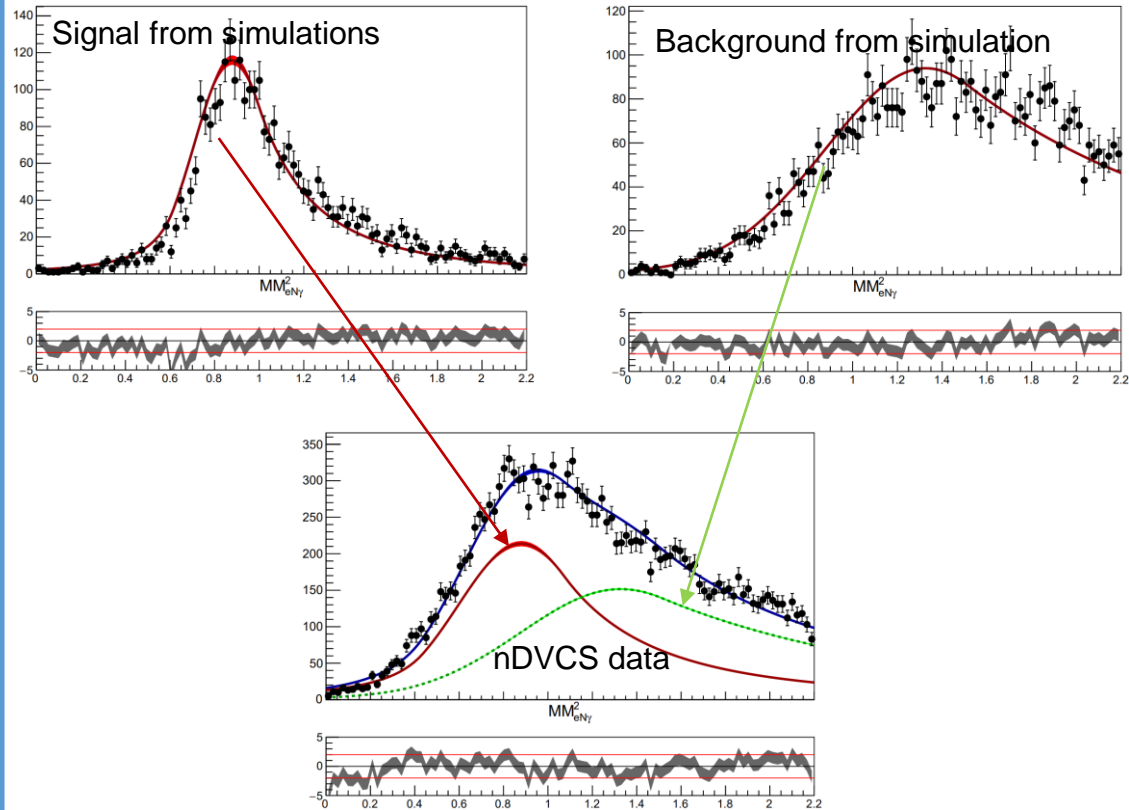
- Subtraction using simulations of the background channel
 - Monte Carlo simulations:
 - GPD-based event generator for DVCS/ π^0 on deuterium
 - DVCS amplitude calculated according to the BKM formalism
 - Fermi-motion distribution evaluated according to Paris potential
- 1. Estimate the ratio of partially reconstructed $eN \pi^0$ (1 photon) decay to fully reconstructed $eN \pi^0$ decays in MC
- 2. This is done for each kinematic bin to minimize MC model dependence
- 3. Multiply this ratio by the number of reconstructed $eN \pi^0$ in data to get the number of $eN \pi^0$ (1 photon) in data
- 4. Subtract this number from DVCS reconstructed decays in data per each kinematical bin

$$\text{Simulations: } R = \frac{N(eN\pi_{1\gamma}^0)}{N(eN\pi^0)}$$

$$\text{Data: } N(eN\pi_{1\gamma}^0) = R * N(eN\pi^0)$$

$$N(DVCS) = N(DVCS_{recon}) - N(eN\pi_{1\gamma}^0)$$

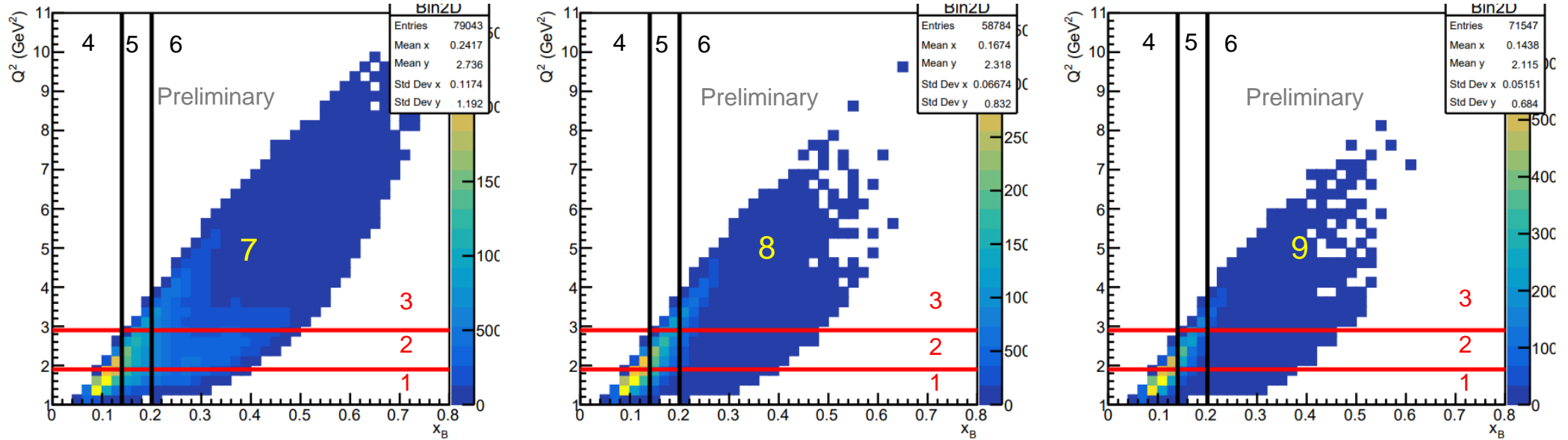
- π^0 background subtraction is also performed by statistical unfolding of contribution to the missing mass spectrum
M. Pivk and F.R. Le Diberder, NIMA 555 1 2005



The difference between the estimations of background from both methods is considered as a systematic



First-time measurement of nDVCS with detection of the active neutron

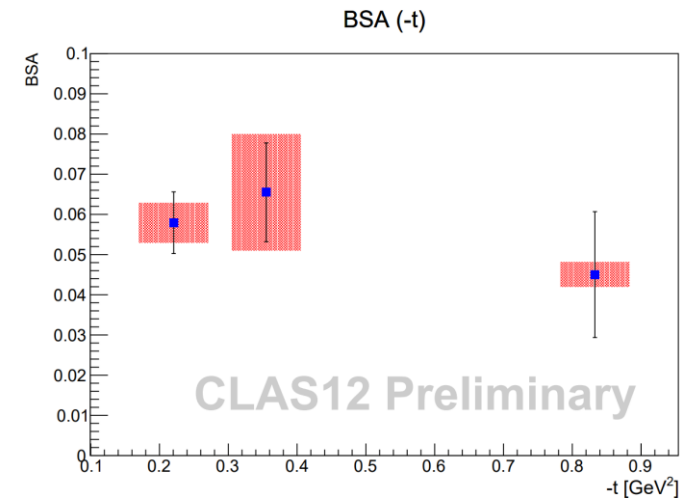
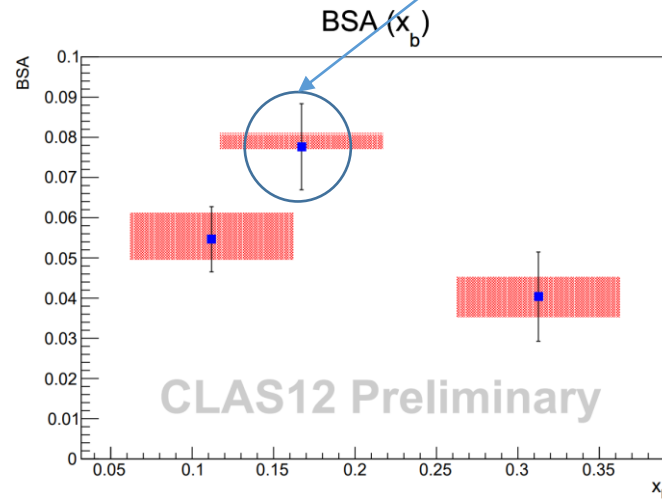
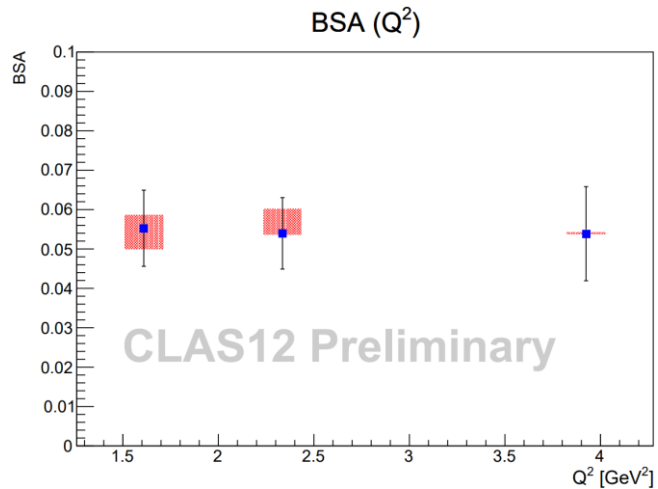
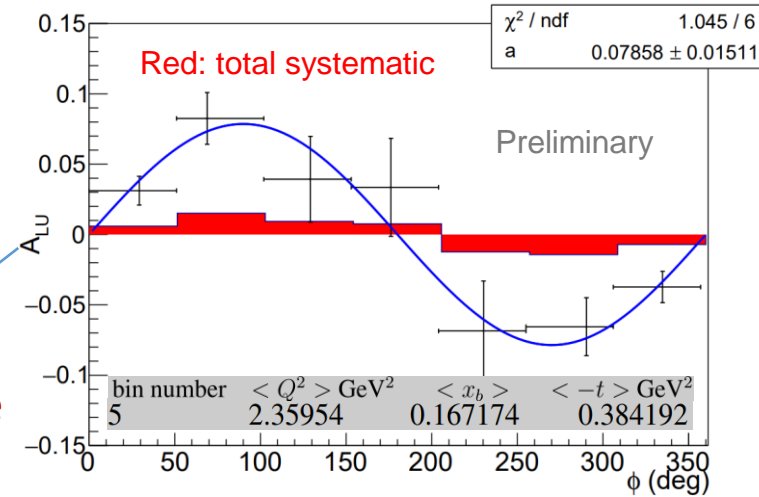


bin number	$\langle Q^2 \rangle$ GeV ²	$\langle x_b \rangle$	$\langle -t \rangle$ GeV ²
1	1.60973	0.132015	0.388061
2	2.33568	0.199322	0.467386
3	3.92472	0.314797	0.667296
4	1.70901	0.111932	0.324567
5	2.35954	0.167174	0.384192
6	3.29066	0.312552	0.70405
7	2.91918	0.277885	0.832902
8	2.44265	0.185242	0.355265
9	2.16854	0.149355	0.22063

- Compared to the previous experiment, CLAS12 provides :
 - The possibility to scan the BSA of nDVCS on a wide phase space
 - The possibility to reach the high Q^2 high x_b region of the phase space
 - Exclusive measurement with the detection of the active neutron
- Hall A @ JLAB: one measured kinematical point at $Q^2=1.9$ GeV² and $x_b=0.36$

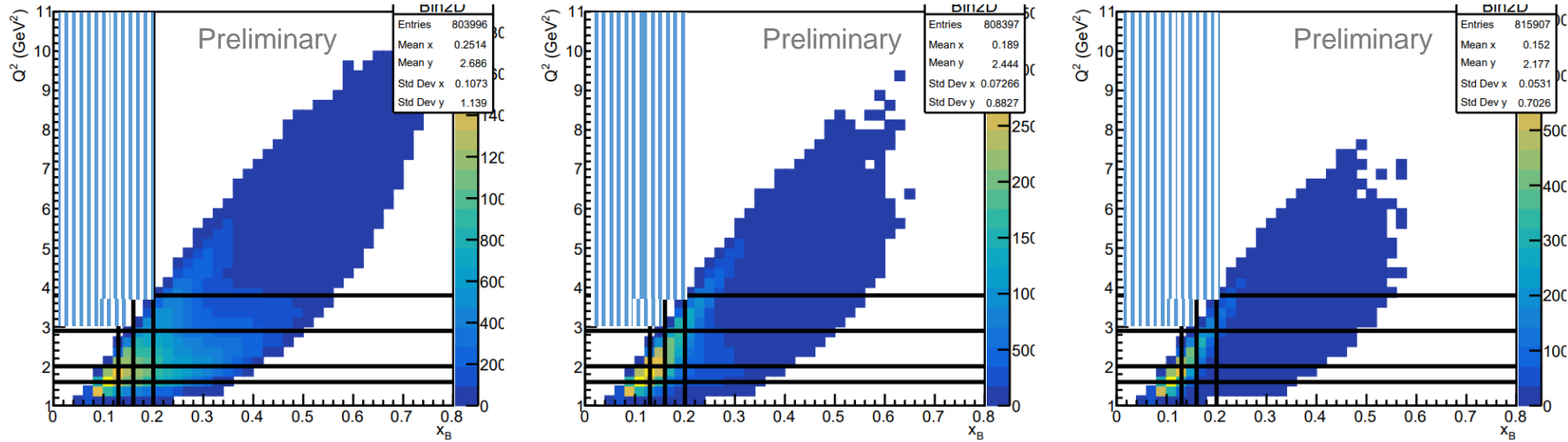


- Observation of positive BSA for nDVCS
- Systematic errors include:
 - Error due to beam polarization
 - Error due to selection cuts
 - Error due to residual proton contamination
 - Error due to merging of data sets with different energies
- Statistics is expected to double with remaining scheduled beam time and improvements with reconstruction software





First-time measurement of incoherent pDVCS on deuteron



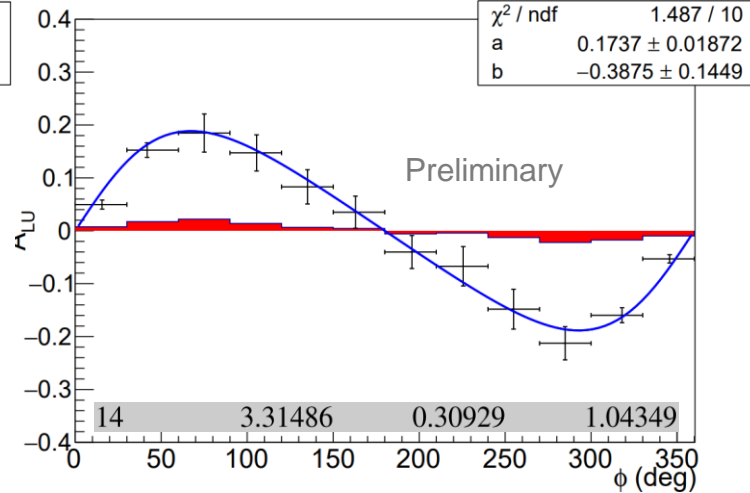
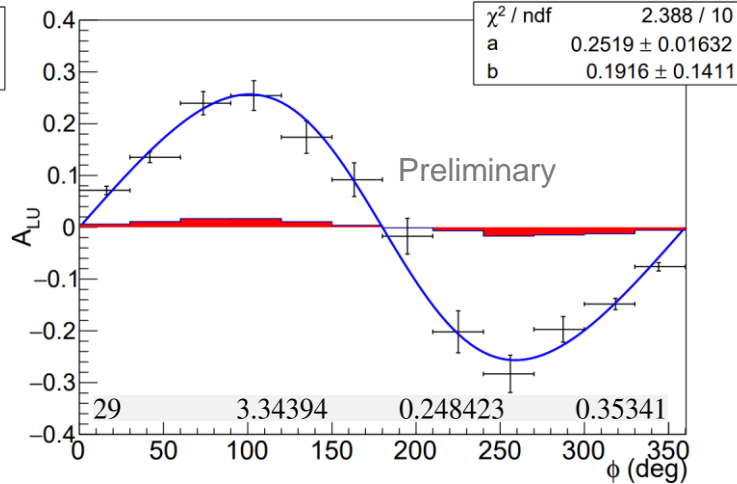
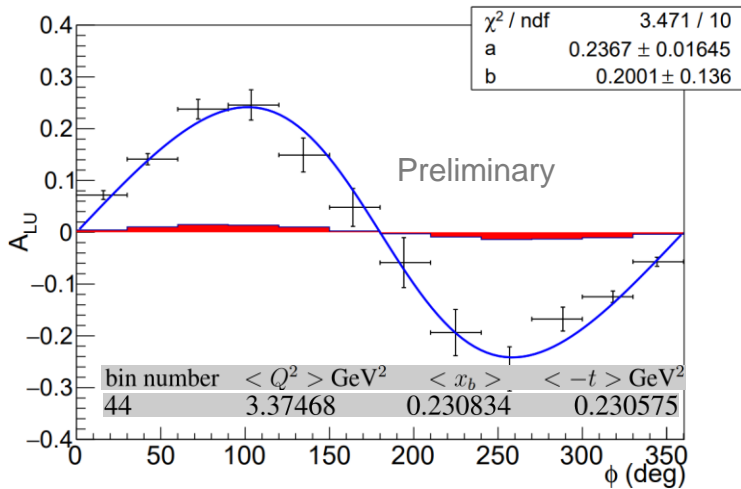
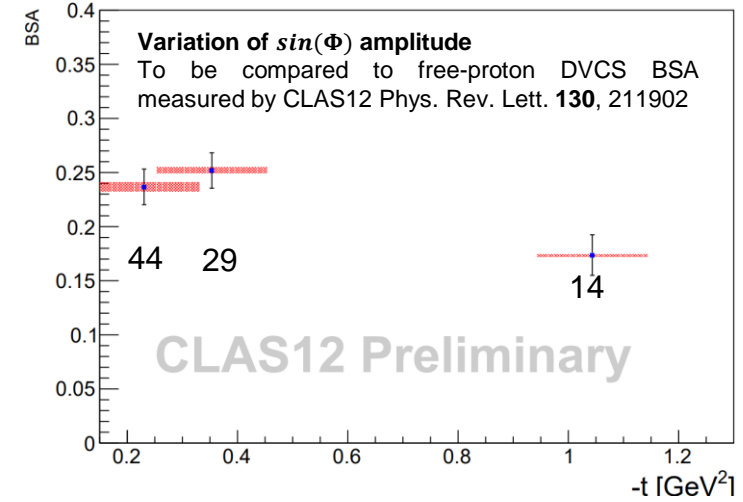
Bin numbering starts from left to right and from bottom up

- Complementary to previous experiment on proton target:
 - Quantify medium effects on GPDs

bin number	$\langle Q^2 \rangle$ GeV ²	$\langle x_b \rangle$	$\langle -t \rangle$ GeV ²
1	1.43794	0.10069	0.767361
2	1.48186	0.144366	0.844629
3	1.4914	0.178824	0.87073
4	1.50756	0.2373	0.851789
5	1.76792	0.114657	0.777427
6	1.8051	0.144373	0.825599
7	1.80447	0.179402	0.863781
8	1.81536	0.258406	0.923301
9	2.0849	0.124705	0.764681
10	2.26532	0.146577	0.793068
11	2.4122	0.179697	0.827414
12	2.43479	0.287563	1.00085
13	3.0799	0.188297	0.790217
14	3.31486	0.30929	1.04349
15	4.83889	0.380624	1.228
16	1.43915	0.100179	0.356721
17	1.49262	0.142616	0.362959
18	1.4954	0.176071	0.350067
19	1.50509	0.249393	0.309281
20	1.77057	0.114679	0.34701
21	1.81394	0.143668	0.348841
22	1.82669	0.175209	0.355866
23	1.81383	0.263491	0.318227
24	2.08646	0.124711	0.342502
25	2.26728	0.146758	0.340636
26	2.46209	0.17752	0.348786
27	2.45997	0.26518	0.340427
28	3.08043	0.188274	0.334151
29	3.34394	0.248423	0.35341
30	4.46623	0.295696	0.370628
31	1.43626	0.0986234	0.200339
32	1.50515	0.13983	0.218898
33	1.49559	0.17749	0.195675
34	1.50618	0.241843	0.211988
35	1.77032	0.114665	0.198266
36	1.83854	0.140417	0.212787
37	1.82375	0.176723	0.20719
38	1.81611	0.248591	0.216637
39	2.08516	0.124803	0.198108
40	2.27128	0.145977	0.203877
41	2.55103	0.174046	0.21458
42	2.44112	0.256179	0.228055
43	3.07532	0.187944	0.210093
44	3.37468	0.230834	0.230575
45	4.30035	0.274016	0.247191



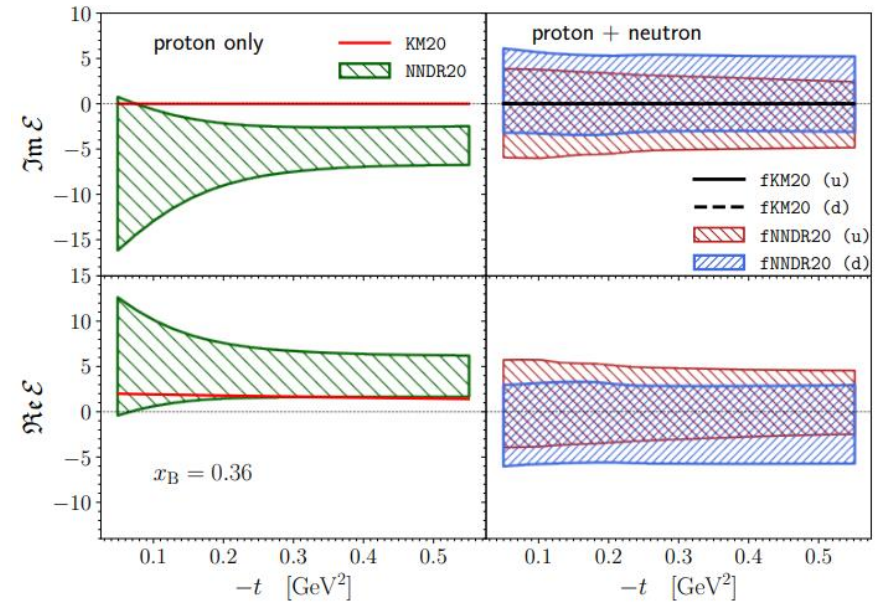
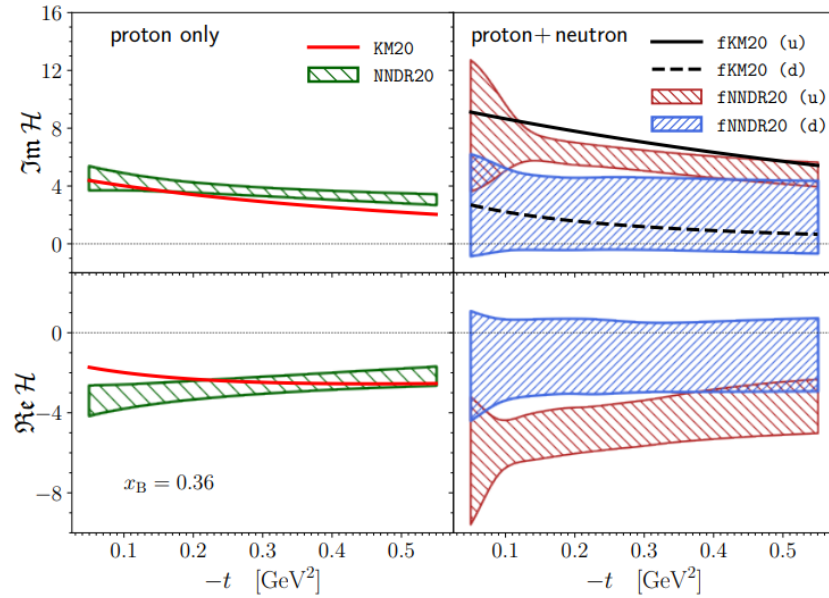
- Systematic errors include:
 - Error due to beam polarization
 - Error due to selection cuts
 - Error due to merging of data sets with different energies
- Statistics is expected to triple with remaining scheduled beam time and improvements with reconstruction software





Impact of new data

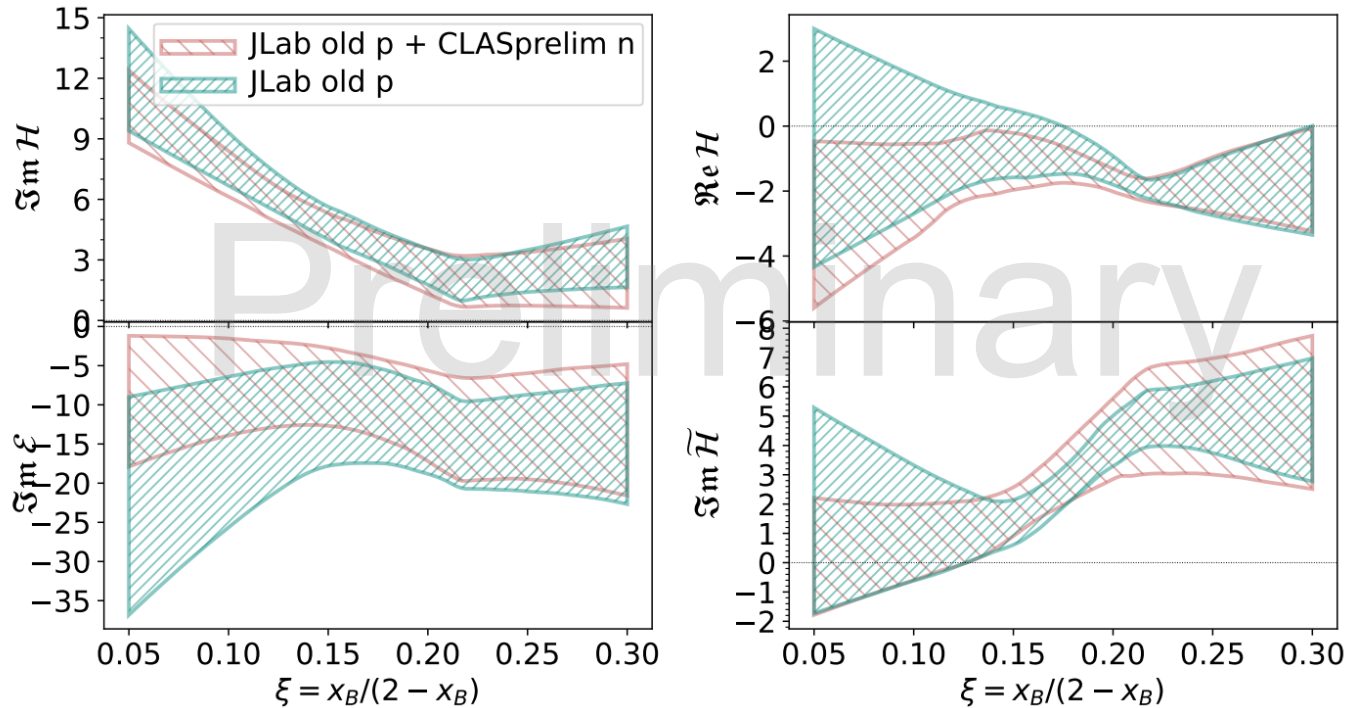
- Previous attempt at flavor separation by M. Čuić, K. Kumerički, A. Schäfer Phys. Rev. Lett. 125 (2020), no. 23 232005



- up and down contributions to CFF H separated
- CFF E cannot be separated



- Train new models with old JLab and new CLAS12 data
 - 40 NN trained on old data and another 40 NN trained on old JLAB pDVCS + new CLAS12 nDVCS data
 - separate models for u and d flavors of CFFs Im H and Im E
 - flavor agnostic (flavor summed) models for CFFs Re H and Im \tilde{H}



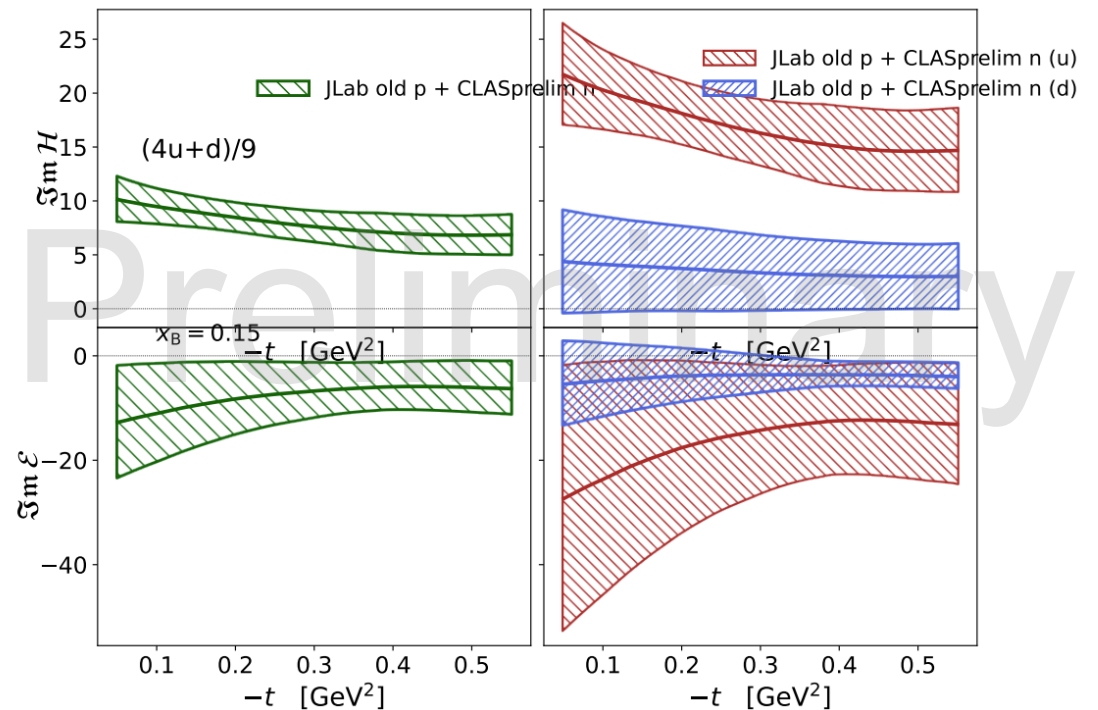
Globally: shift and reduction of uncertainty more evident in Im E



- Train new models with old JLab and new CLAS12 data
 - 40 NN trained on old data and another 40 NN trained on old JLAB pDVCS + new CLAS12 nDVCS data
 - separate models for u and d flavors of CFFs $\text{Im } H$ and $\text{Im } E$
 - flavor agnostic (flavor summed) models for CFFs $\text{Re } H$ and $\text{Im } \tilde{H}$

Flavor separation of $\text{Im}H$ is better than before

Less evident Flavor separation of $\text{Im } E$





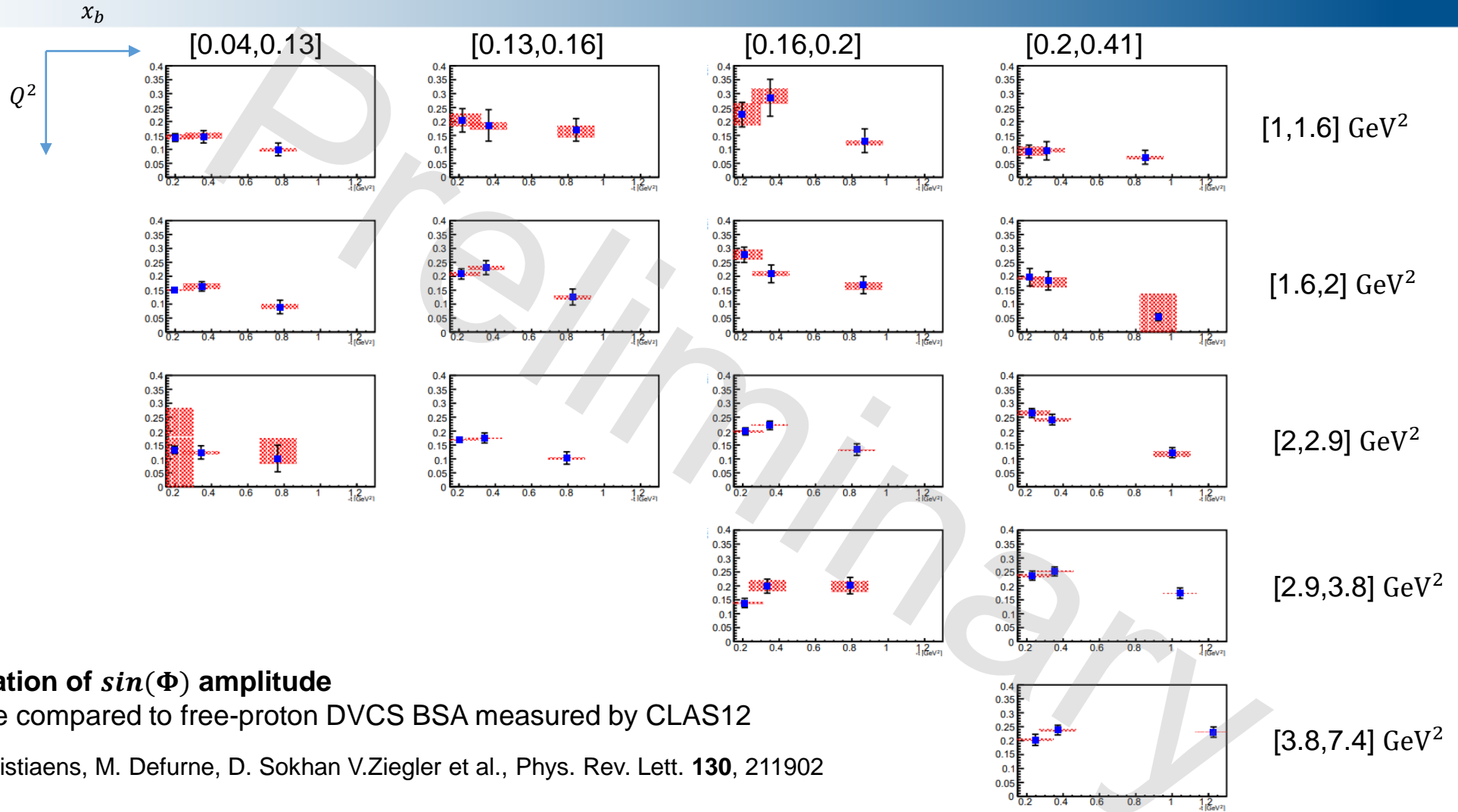
Summary

- GPDs are powerful tool to explore the structure of the nucleons and nuclei
 - Nucleon tomography, quark angular momentum, distribution of forces in the nucleon
- Exclusive reactions can provide important information on nucleon structure
 - DVCS via the extraction of GPDs
- CLAS12 offers a wide kinematical reach over which the GPDs dependence on different kinematical variables can be scanned
 - Data to add constraints on GPDs in unexplored regions of the phase space
 - Possibilities to measure new observables using different experimental configurations
 - Flavor separation of GPDs
- Promising results from incoherent DVCS on deuteron (n and p channels) from CLAS12 data
 - First BSA measurement from neutron-DVCS with tagged neutron
 - First measurement of BSA for proton-DVCS with deuterium target
 - To be compared to free-proton DVCS BSA measured by CLAS12

G. Christiaens, M. Defurne, D. Sokhan V.Ziegler et al., arXiv (2022) 221111274.



Backup slides



Variation of $\sin(\Phi)$ amplitude

To be compared to free-proton DVCS BSA measured by CLAS12

G. Christiaens, M. Defurne, D. Sokhan V.Ziegler et al., Phys. Rev. Lett. **130**, 211902